Articles

Peroxynitrite and Nitric Oxide Differently Target the Iron−Sulfur Cluster and Amino Acid Residues of Human Iron Regulatory Protein 1†

Emmanuelle Soum,‡ Xavier Brazzolotto,§ Charilaos Goussias,|| Cécile Bouton,‡ Jean-Marc Moulis,§ Tony A. Mattioli,|| and Jean-Claude Drapier*,‡

Institut de Chimie des Substances Naturelles, CNRS, 91190 Gif-sur-Yvette, France, Département Réponse et Dynamique Cellulaires, CEA/Grenoble, 38054 Grenoble, France, and Laboratoire de Biophysique du Stress Oxydant, Section de Bioénergétique, Département de Biologie Joliot Curie, CEA/Saclay, 91191 Gif-sur-Yvette cedex, France

Received February 18, 2003; Revised Manuscript Received May 7, 2003

ABSTRACT: Iron regulatory protein 1 (IRP1) is a redox-sensitive protein which exists in two active forms in the cytosol of eukaryotic cells. Holo-IRP1 containing a [4Fe-4S] cluster exhibits aconitase activity which catalyzes the isomerization of citrate and isocitrate. The cluster-free protein (apo-IRP1) is a transregulator binding to specific mRNA, and thus post-transcriptionally modulating the expression of genes involved in iron metabolism. The resonance Raman (RR) spectra of human recombinant holo-IRP1 (rhIRP1) excited at 457.9 nm show that the 395 cm^{-1} band, attributed to a terminal Fe−S stretching mode of the cluster, is replaced by a 405 cm^{-1} band, consistent with the conversion of the $[4Fe\text{-}4S]^{2+}$ center to a $[3Fe\text{-}4S]^{+}$ center, upon exposure to peroxynitrite. This conclusion was confirmed by electron paramagnetic resonance (EPR) data and correlated with the loss of aconitase activity. In another series of experiments, the RR spectra also revealed the presence of additional bands at 818 and 399 cm^{-1} when rhIRP1 was treated with a peroxynitrite synthesized by a different procedure. These bands correspond to those of 3-nitrotyrosine, and they indicate nitration of at least one tyrosine residue in rhIRP1. This was further confirmed by Western blot analysis with an anti-nitrotyrosine antibody. In contrast, the reaction of rhIRP1 with NO in the absence of oxygen revealed full mRNA binding activity of the protein, without nitration of tyrosines. These results strongly suggest that NO mainly acts as a regulator of IRP1 whereas peroxynitrite is likely to disrupt the IRP1/IRE regulatory pathway.

Iron homeostasis is essential to mammalian cell functions such as oxygen uptake, proliferation, and energetic metabolism. Yet the status of cellular iron levels is double-edged: cells must acquire sufficient iron for metabolic needs, and at the same time, they must minimize excess redox-active iron which could lead to the formation of reactive oxygen species via Fenton chemistry (*1*). Iron regulatory proteins (IRP1[1] and IRP2) play an important role in modulating cellular iron levels by regulating the expression of ferritin and transferrin receptor whose mRNAs contain a specific stem−loop structure, called the iron responsive element (IRE), in their untranslated regions. Upon binding to IRE-(s), IRPs repress ferritin translation and, conversely, stabilize transferrin receptor mRNA (*2*). IRP1, whose steady state concentration is usually higher than that of IRP2, also exhibits an enzymatic activity converting citrate to isocitrate in the cytosol, just as mitochondrial aconitase does in the Krebs cycle. Like the other members of the aconitase family, IRP1 (the cytosolic aconitase) is a metalloprotein possessing a [4Fe-4S] cluster that binds the substrate (*3*) and which is found in a region of the protein overlapping with the RNA binding domain. This [4Fe-4S] cluster differs from most other such clusters with complete cysteine ligation by having one iron (Fe_a) coordinated by oxygen atom(s) from water or (iso)-citrate molecules, the natural substrate of aconitases. The [4Fe-4S] prosthetic group is thus required for aconitase activity and maintains the protein in a specific folded conformation which disables the RNA binding capacity of the protein.

Biosynthesis of NO activates IRP1 by inhibiting its aconitase function and enhancing its regulatory function (*4*, *5*). Regulation by NO has been largely documented (*6*, *7*),

† This work was supported in part by the Association pour la Recherche contre le Cancer (Grant 5856) and by GDR 1879 (CNRS). T.A.M. acknowledges financial support from the Regional Council of the Ile-de-France for an equipment grant (SESAME). C.G. is supported by a Marie Curie individual fellowship (MCFI-2000-00611).

* To whom correspondence should be addressed: Institut de Chimie des Substances Naturelles, CNRS, 91190 Gif-sur-Yvette, France. Telephone: 33 1 69 82 45 62. Fax: 33 1 69 07 72 47. E-mail: Jean-Claude.Drapier@icsn.cnrs-gif.fr.

‡ CNRS.

§ CEA/Grenoble.

|| CEA/Saclay.

[1] Abbreviations: 2-ME, 2-mercaptoethanol; BSA, bovine serum albumin; CCD, charge-coupled device; EPR, electron paramagnetic resonance; IRP, iron regulatory protein; NO, nitric oxide; $ONOO^-$, peroxynitrite; RR, resonance Raman; SIN-1, 3-morpholinosydnonimine; TBST, Tris-buffered saline with 0.1% Tween-20.

10.1021/bi030041i CCC: $25.00
Published on Web 06/03/2003

but whether NO itself or a product derived from NO, such as peroxynitrite, is the effector molecule has been debated (*8*−*10*). With respect to peroxynitrite, there is a consensus view that it induces loss of aconitase activity of both mitochondrial aconitase and IRP1, but it is still unclear whether peroxynitrite activates the regulatory function of IRP1 (*11*−*13*). We previously found that peroxynitrite could inhibit aconitase activity of IRP1 *in vitro* without enhancing its capacity to bind mRNA (*12*). We proposed that peroxynitrite converts IRP1 to an oxidized apoprotein without any activity, most likely because two cysteine ligands, including Cys 437, were exposed to oxidation by cluster removal (*12*). Recently, it was reported that SIN-1, a chemical which releases peroxynitrite spontaneously in the presence of oxygen, reduces the capacity of cluster-free IRP1 to bind IRE but, at low concentrations, converts the holoprotein (aconitase) to IRE-binding IRP1 (*13*).

To characterize further the role peroxynitrite may play in IRP1 activity, we have studied purified recombinant human IRP1 (rhIRP1) and analyzed its post-translational modifications using resonance Raman (RR) and electron paramagnetic (EPR) spectroscopies in combination with biological activity determinations after exposure to peroxynitrite solutions prepared according to two frequently used methods. RR spectroscopy is well-suited to the study of structural properties and specific modifications of Fe−S cluster proteins. It can also be used to detect chemical alterations on specific amino acid residues in proteins, e.g., nitration of tyrosines (*14*). Under pathophysiological conditions, including ischemia/reperfusion, neurodegenerative diseases and atherosclerosis (*15*), peroxynitrite-promoted nitration of tyrosine residues on proteins has become a classical marker of nitrogen oxide-related diseases (*16*, *17*). Moreover, an alternative pathway for biological formation of nitrotyrosine was recently described, involving peroxidase-, heme-, or iron-catalyzed oxidation of nitrite, an end product of NO (*18*−*20*). In both cases, the nitrating species is presumably the nitrogen dioxide radical ($NO_2^{\bullet}$). It was thus also important to clarify the role of nitration in the aconitase−IRE-binding protein switch.

The RR spectra of the iron−sulfur cluster of mitochondrial aconitase, in both the $[4Fe\text{-}4S]^{2+}$ and $[3Fe\text{-}4S]^{+}$ forms, have been previously reported by Spiro and co-workers (*21*). To date, no such studies have yet been reported for human IRP1. In this contribution, the RR spectra of $[4Fe\text{-}4S]^{2+}$ rhIRP1 are presented, and spectroscopic evidence that conversion of this cluster to a $[3Fe\text{-}4S]^{+}$ form occurs upon exposure to peroxynitrite is provided. Resultant loss of aconitase activity is not strictly correlated with peroxynitrite-induced tyrosine nitration. We also show that some of these features differ from those resulting from the reaction of rhIRP1 with nitric oxide.

MATERIALS AND METHODS

Preparation of Pure Recombinant Human IRP1 (rhIRP1). rhIRP1was expressed in *Escherichia coli* K38/pGP1-2 transformed with the plasmid pT7-7-hIRP1 and purified under anaerobic conditions as described previously (*22*). Purified rhIRP1 was in 20 mM Tris-HCl (pH 7.4) with 0.2 mM citrate. The concentration of rhIRP1 was evaluated spectrophotometrically using the Bio-Rad protein assay with bovine serum albumin (BSA) as a standard. The values obtained with this assay agreed with those calculated for holo-IRP1 taking an ϵ_{400} of 16 000 M^{-1} cm^{-1}. For RR experiments, the protein was concentrated to 1 mM by using membrane microconcentrators (Centricon 30K, Amicon).

Peroxynitrite Synthesis and rhIRP1 Treatment. Two different stock solutions of peroxynitrite, termed solutions A and B for convenience, were used. Solution A was prepared using a modified method described by Beckman et al. (*23*). Briefly, 1 M H_2O_2 in 1.75 M HNO_3, 1 M $Na^{14}NO_2$ or $Na^{15}NO_2$, and 6 N NaOH were rapidly mixed in two steps in a home-built tubing system, leading to a cold recipient containing a magnetic stirrer kept on ice. The concentrations of peroxynitrite solutions thus synthesized (170−190 mM) were measured spectrophotometrically at 302 nm (ϵ_{302} = 1670 M^{-1} cm^{-1}) after dilution in 0.1 N NaOH (*17*). Nitrite contamination was evaluated by using Griess reagent after the peroxynitrite solution had been diluted in a 100 mM potassium phosphate buffer (pH 4.5) to convert peroxynitrite into nitrates exclusively (*24*). Only 1−5% of the total nitrites were present in the $O^{14}NOO^-$ or $O^{15}NOO^-$ solution. The H_2O_2 concentration was determined according to the method of Pick and Keisari (*25*), and showed that the H_2O_2:peroxynitrite ratio was less than 1:50. For treatment with solution A, rhIRP1 (10 μM) was incubated with 500 μM $O^{14}NOO^-$ or $O^{15}NOO^-$, in 100 mM Hepes (pH 7.4) for 30 min at 20 °C. After reaction, samples were concentrated to 1 mM for RR experiments. Solution B of peroxynitrite was synthesized using H_2O_2 and isoamyl nitrite (*26*). The resulting peroxynitrite solution was treated with MnO_2 to eliminate H_2O_2 (*20*), and the peroxynitrite concentration (1−2 M) was determined spectrophotometrically at 302 nm. Nitrites were quantified at acidic pH as described above, and found to be at high levels (≥50% as compared to the level of peroxynitrite). Concentrated rhIRP1 (1 mM) was then exposed to peroxynitrite after addition of solution B at a ratio of 1:30. "Decomposed" peroxynitrite solutions were prepared by adding a solution (A or B) to the appropriate buffer solution, and the contents were left to decompose in aqueous buffer prior to addition of rhIRP1. In all cases, the addition of the decomposed peroxynitrite solution produced no observable changes in aconitase or mRNA binding activity, or in the RR spectrum of the cluster, nor did it result in observable nitration of the protein, as determined by Western blot and RR procedures described below.

Addition of NO to rhIRP1. Diethyldiammonium (*Z*)-1-(*N*,*N*-diethylamino)diazen-1-ium-1,2-diolate (DEA-NO, Cayman Chemical, Ann Arbor, MI) was used as the NO donor. In an anaerobic glovebox ensuring an oxygen level of <2 ppm, a 0.18 M stock solution was prepared in 0.1 M bis-tris-propane (pH 9). Then 0.9 μmol DEA−NO species was mixed with 40 nmol (holo)rhIRP1 and left to react for 45 min at 29 °C. Since the half-life of the DEA−NONOate form is on the order of 2 min at neutral pH, a 50-fold excess of NO per rhIRP1 is expected to be rapidly produced under these conditions. After reaction, the protein was desalted and concentrated using Microcon YM50 membranes (Amicon).

Aconitase Activity. Aconitase activity of rhIRP1 was determined as described (*27*), by measuring the decrease in *cis*-aconitate absorbance using a spectrophotometer equipped with a thermostated multicuvette holder (Safas, Monaco). Specific aconitase activity was quantified using the molar

extinction coefficient of *cis*-aconitate at 240 nm ($\epsilon_{240} = 3600$ M^{-1} cm^{-1}).

Electrophoretic Mobility Shift Assay (EMSA). The IRE binding activity of untreated (control) or peroxynitrite-treated rhIRP1 was quantified as described previously (*27*, *28*). Briefly, 2 ng of rhIRP1 was incubated with a molar excess of ^{33}P-labeled ferritin IRE probe in a final volume of 20 μL of 10 mM Hepes (pH 7.6), 40 mM KCl, 3 mM $MgCl_2$, 5% glycerol, and 50 μg/mL bovine serum albumin. After incubation for 20 min at room temperature, 1 μL of RNase T1 (1 unit/μL) was added, and samples were incubated for 10 min at room temperature before addition of 2 μL of 50 mg/mL heparin for an additional 10 min. IRE−IRP1 complexes were resolved on a nondenaturing 6% acrylamide gel and quantified as radioactive bands with ImageQuant software (Molecular Dynamics). Treatment of IRP1 with 2% mercaptoethanol (2-ME) allows conversion of every form of IRP1 to reduced apo-IRP1 which is able to bind IREs, and therefore corresponds to the total binding activity of the protein.

Detection of Nitrated rhIRP1. The presence of nitrotyrosine was assessed by Western blot analysis. Protein rhIRP1, exposed or not exposed to peroxynitrite, was resolved on an 8% SDS−polyacrylamide gel and then transferred to a nitrocellulose membrane (Hybond ECL, Amersham Pharmacia Biotech). The membrane was saturated in a Tris-buffered saline solution [100 mM Tris and 137 mM NaCl (pH 7.6)] with 0.1% Tween-20 (TBST) containing 5% dry milk at 37 °C for 1 h, followed by an overnight incubation with a monoclonal anti-nitrotyrosine mouse antibody (Cayman Chemical) at 4 °C in TBST. After several washes, the membranes were probed with a peroxidase-conjugated goat anti-mouse secondary antibody in TBST for 45 min at room temperature. Membranes were then washed, and the immunoreactive proteins were detected by chemiluminescence (SuperSignal, Pierce Chemicals, Rockford, IL). In some experiments, membranes were stripped and reprobed with a polyclonal anti-IRP1 antibody as described elsewhere (*29*) to check equal loading.

RR Spectroscopy. RR spectra were recorded using a modified single-stage spectrometer (Jobin-Yvon T64000) equipped with a back-thinned CCD detector. Stray scattered light was rejected using a holographic notch filter (Kaiser Optical Systems). Laser excitation at 457.9 or 496.5 nm was provided by an argon laser (Coherent Innova 100), with 80 mW power at the sample which was held in a cold He gas circulating cryostat (Janis Research Co., STV-100, Wilmington, MA) maintained at 15 K. The sample (1 μL, 1 mM in protein) was deposited on a glass slide mounted within the cryostat in a 135° back-scattering geometry with respect to the incident laser beam and the collection lens of the spectrometer. Spectra were recorded by the co-addition of 100 individual spectra with an exposure time of 5 s each (the total accumulation time was ca. 10 min). Final reported Raman spectra represent the average of several such 10 min spectra. Averaging and baseline correction were performed using GRAMS 32 (Galactic Industries, Salem, NH). Spectral resolution was better than 5 cm^{-1}.

EPR Spectroscopy. For the EPR experiments, aliquots of the RR samples (1 mM) were diluted to a concentration of 10 μM in 100 mM Tris-HCl (pH 7.4) and frozen in liquid N_2. X-band EPR spectroscopy was performed using a Bruker ER-300 spectrometer, equipped with an Oxford ESR 9 cryostat, a Hewlett-Packard 5350B frequency counter, and a Bruker 035M NMR gaussmeter.

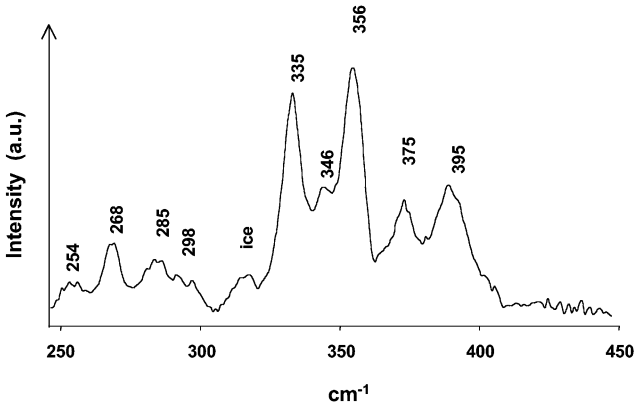

FIGURE 1: RR spectra of [4Fe-4S] rhIRP1. rhIRP1, purified as the [4Fe-4S] form, was concentrated to 1.2 mM in 50 mM Tris (pH 7.4), and its RR spectrum was recorded at 15 K with the following parameters: laser excitation of 457.9 nm, laser output power of 100 mW, spectral bandwidth of ca. 5 cm^{-1}, and precision of ± 1 cm^{-1}.

RESULTS

RR Spectra of rhIRP1. The room-temperature UV−visible absorption spectrum of the holo-rhIRP1 protein exhibits a broad, unresolved envelope of several bands centered at ca. 400 nm (*22*) which typically contains the contributions of the $S \rightarrow Fe^{3+}$ charge transfer bands of the $[4Fe\text{-}4S]^{2+}$ cluster. Figure 1 shows the low-temperature (15 K) RR spectrum of rhIRP1 in the $[4Fe\text{-}4S]^{2+}$ cluster form, excited at 457.9 nm, which results in the resonance enhancement of the Fe−S vibrational modes of the cluster. Much work, in the form of selective isotopic substitutions and normal mode calculations (*30*−*32*), has been done to assign vibrational modes of [4Fe-4S]. The 335 cm^{-1} (A_1 in tetrahedral T_d symmetry terminology; mode assignments and analysis for these clusters are based on their approximate tetrahedral symmetry) and 395 cm^{-1} (T_2) bands are assigned to Fe−S bridging vibrational modes, while the 346 (T_2), 356 (T_2), and 375 cm^{-1} (T_2) bands are assigned to Fe−S terminal vibrational modes. The weaker, lower-frequency bands observed at 254 (T_2), 268 (E), 285 (E), and 298 cm^{-1} (T_1) are also due to Fe−S bridging modes.

In addition to the cluster vibrational modes, spectra of rhIRP1 display bands at 464 and 1660 cm^{-1} (not shown) that have also been observed with mitochondrial aconitase and that were tentatively assigned to vibrational modes of an asparagine side chain hydrogen bonded and coupled to the cluster (*21*). These common spectroscopic features emphasize the structural resemblance of the Fe−S cluster of the rhIRP1 sample studied here with mitochondrial aconitase recorded under similar conditions (*21*, *33*). In both cases, the implemented RR conditions do not yield contributions from Fe−O vibrations, a point previously addressed by Spiro and co-workers regarding mitochondrial aconitase (*21*). The spectra also indicate that the absence of cysteine coordination on the fourth iron atom, Fe_a, does not significantly alter the vibrational pattern of the [4Fe-4S] cluster, in particular, the bridging modes. In brief, comparison of these data with the existing literature indicates that the low-

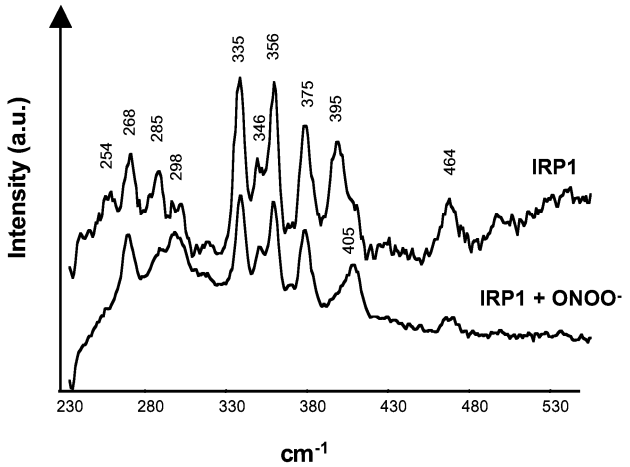

FIGURE 2: Conversion of $[4Fe\text{-}4S]^{2+}$ into a $[3Fe\text{-}4S]^{+}$ rhIRP1 by peroxynitrite (solution A). rhIRP1 (10 μM) was exposed to peroxynitrite (500 μM) in 100 mM Hepes (pH 7.4) at 20 °C. After 30 min, control or peroxynitrite-treated rhIRP1 was concentrated to 1 mM, and RR spectra were recorded as described in the legend of Figure 1.

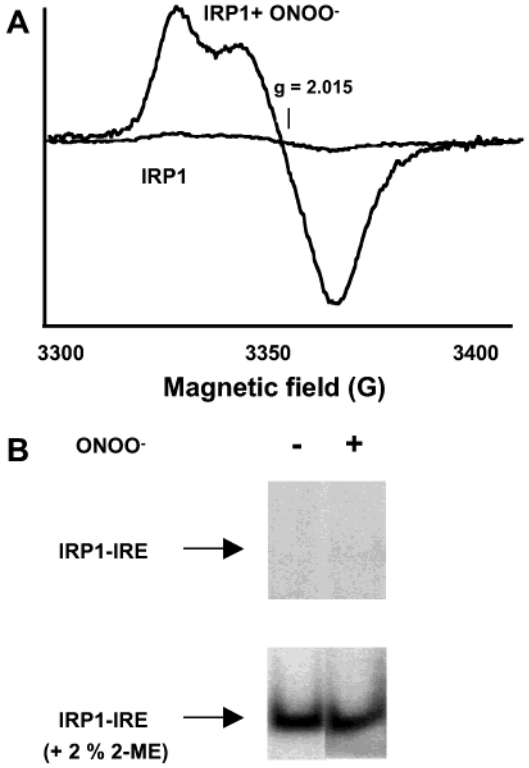

FIGURE 3: (A) The EPR spectra of the same samples as described in the legend of Figure 2 were recorded at 15 K after dilution (10 μM) and freezing in liquid nitrogen: microwave frequency of 9.436 GHz, modulation frequency of 100 kHz, modulation amplitude of 4G, and microwave power of 100 μW. (B) rhIRP1 IRE binding activity was also assessed by a band shift assay, including in the presence of 2% 2-mercaptoethanol to assess full activity.

frequency range RR spectra of aconitase/IRP1, encompassing the Fe−S modes, closely resemble those of other [4Fe-4S] cluster proteins with complete terminal cysteine coordination on the four iron atoms (*21*, *33*).

RR Spectra of Peroxynitrite (solution A)-Treated rhIRP1. In preliminary experiments, we verified that the addition of decomposed (see Materials and Methods) peroxynitrite did not modify either the aconitase activity of rhIRP1 or the RR spectrum of the cluster, as observed using 457.9 nm excitation (not shown). In contrast, significant differences were observed in the RR spectrum of rhIRP1 treated with freshly prepared peroxynitrite of solution A (Figure 2). Although many bands of the Fe−S modes were still observed in the 250−400 cm^{-1} spectral range, the bands of $[4Fe\text{-}4S]^{2+}$ rhIRP1 at 254, 285, and 395 cm^{-1} experienced large intensity decreases or disappeared entirely. In addition, a new band at 405 cm^{-1} was observed. This new pattern of RR bands is very similar to that observed for the $[3Fe\text{-}4S]^{+}$ cluster of mitochondrial aconitase (*21*). The replacement of the 395 cm^{-1} mode with one above 400 cm^{-1} is a strong sign of the conversion of the cluster from the $[4Fe\text{-}4S]^{2+}$ form to the $[3Fe\text{-}4S]^{+}$ form. Taken together, the above RR results clearly indicate that the Fe−S cluster of IRP1 has undergone a $[4Fe\text{-}4S]^{2+}$ to $[3Fe\text{-}4S]^{+}$ conversion. Interestingly, samples similarly treated with either ^{14}N- or ^{15}N-enriched peroxynitrite displayed spectra that were identical, with no evidence of isotopic shifts for bands between 250 and 400 cm^{-1} (not shown). Thus, RR spectroscopy does not provide evidence for nitrogen binding (from peroxynitrite or derivatives) to the $[3Fe\text{-}4S]^{+}$ cluster of rhIRP1. This observation is entirely consistent with full cysteine coordination for a [3Fe-4S] cluster.

EPR Spectroscopy of Peroxynitrite (solution A)-Treated rhIRP1. To establish firmly the conversion of the aconitase active center into a $[3Fe\text{-}4S]^{+}$ cluster, the same sample was analyzed by EPR at 15 K. Figure 3A shows the $g \approx 2$ region of the EPR spectrum of peroxynitrite-treated rhIRP1 with a single, slightly rhombic g signal centered at 2.015. Such features are fully consistent with the presence of a $[3Fe\text{-}4S]^{+}$ center (*3*). The monotonic decrease in the intensity of the $g = 2.015$ signal in peroxynitrite-treated rhIRP1 with increasing temperatures until signal cancellation above 30 K indicates that a single paramagnetic species was present in this sample, without any sign of a signal arising from a reduced, $[4Fe\text{-}4S]^{+}$, or oxidized, $[4Fe\text{-}4S]^{3+}$, cluster.

Biological Assays of Peroxynitrite (solution A)-Treated rhIRP1. Aconitase activity and the capacity of the protein to bind mRNA were monitored in parallel with the Raman experiments. Aconitase activity was essentially completely lost (96% inhibition) after treatment with peroxynitrite. However, no increase in RNA binding activity was observed (Figure 3B). Full RNA binding activity, similar for peroxynitrite-treated and untreated samples, was obtained only with 2% 2-Me (Figure 3B, bottom panel). To assess further the extent of protein modification in these experiments with peroxynitrite, the possible nitration of tyrosine residues was investigated by Western blot, with an anti-nitrotyrosine antibody. Nitrotyrosine was not significantly detectable, and only a faint band was visible after a long-term exposure to the chemiluminescent reagent (not shown).

Post-Translational Modifications of rhIRP1 by Peroxynitrite (solution B). We decided to corroborate our result with another preparation of peroxynitrite synthesized by an alternative standard method. Therefore, in a second set of experiments, peroxynitrite (solution B) was prepared according to Uppu et al. (*26*) and, this time, was made devoid of H_2O_2. In this series of experiments, 1 mM rhIRP1 was exposed to a 30-fold excess of peroxynitrite for 30 min. Aconitase activity was essentially completely lost (98% inhibition), and again, no evidence of enhanced mRNA

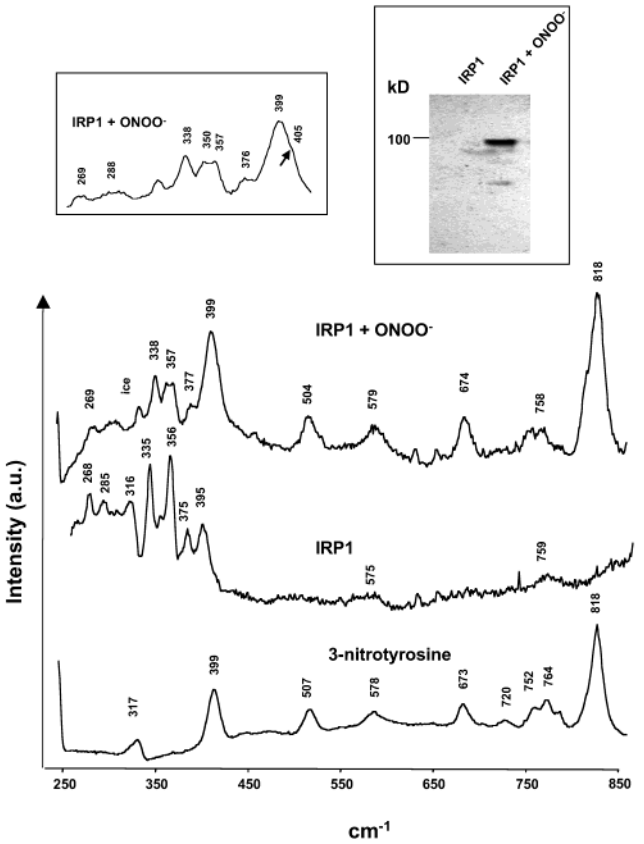

FIGURE 4: Nitration of rhIRP1 exposed to peroxynitrite (solution B). RR spectra (15 K) were recorded with 1 mM rhIRP1. The protein was either untreated (control, middle trace) or treated (top trace) with peroxynitrite solution B (1:30 ratio) for 30 min at 20 °C. A close-up view of the latter is shown in the top left inset. Conditions: laser excitation of 457.9 nm, laser output power of 100 mW, spectral bandwidth of ca. 5 cm^{-1}, and precision of ± 1 cm^{-1}. Western blot analysis was performed with a monoclonal anti-nitrotyrosine antibody (top right inset).

binding was found (not shown). As shown in Figure 4, the RR spectrum of rhIRP1 treated with peroxynitrite still exhibited Raman bands of the Fe−S stretching modes below 400 cm^{-1}. However, several new bands, which were not seen in the spectrum of rhIRP1 exposed to decomposed peroxynitrite or to peroxynitrite solution A (not shown), were observed above 400 cm^{-1} in the spectra of peroxynitrite solution B-treated rhIRP1. Such a pattern of numerous new bands distributed over a large frequency range has never been observed as arising from the vibrational modes of an Fe−S cluster, and they must have another origin. Modification of a protein side chain was suspected, and we decided to probe nitration of tyrosine residue(s). 3-Nitrotyrosine exhibits a broad and relatively intense electronic absorption band at 423 nm that gives rise to resonance of the Raman modes of the nitrotyrosine chromophore within the protein, as is illustrated in an RR study of nitrotyrosine in cytochrome *c* (*14*). Thus, using a properly chosen excitation wavelength, one can simultaneously monitor the state of the Fe−S cluster as well as the presence of nitrotyrosine in the rhIRP1 protein with the same RR data. For example, 457.9 nm excitation ensures both resonance enhancement of the cluster and the preresonance enhancement of nitrotyrosine absorbing at ca. 420 nm.

Figure 4 (bottom trace) shows the preresonance Raman spectrum of 3-nitrotyrosine at pH 7.4, using 457.9 nm excitation. This spectrum exhibits a strong band at 818 cm^{-1} assigned to an NO_2 bending mode of 3-nitrotyrosine (*34*). There is also a relatively weaker band at 399 cm^{-1} which most likely corresponds to a C−N or C−C torsional mode (*34*). These two Raman features, along with the other minor Raman bands, closely match those appearing in the RR spectrum of peroxynitrite solution B-treated rhIRP1 using the same excitation wavelength (i.e., 457.9 nm). The 399 cm^{-1} band is similar in frequency to the 405 cm^{-1} band observed for the $[3Fe\text{-}4S]^+$ cluster in Figure 2. However, its relative intensity, as compared to the rest of the Fe−S cluster modes, is far too large to arise from a cluster mode. Rather, it is approximately one-half the intensity of the 818 cm^{-1} band of nitrotyrosine, a ratio similar to that observed for the preresonance Raman spectrum of 3-nitrotyrosine. Thus, the 399 cm^{-1} band should primarily arise from the nitrotyrosine of the protein and may mask the relatively weaker 405 cm^{-1} band of the [3Fe-4S] cluster. Interestingly, there is a conspicuous shoulder at ca. 405 cm^{-1} on the high-frequency side of the 399 cm^{-1} band in the spectra of peroxynitrite-treated rhIRP1 arising from the [3Fe-4S] cluster (marked with an arrow in Figure 4, left inset). EPR spectroscopy also confirmed the presence of this paramagnetic cluster (not shown). Nitration of tyrosine residues was confirmed by a parallel Western blot experiment performed with an anti-nitrotyrosine antibody. In this set of experiments, a strong signal was easily detected (Figure 4, right inset).

Post-Translational Modifications of rhIRP1 by NO. To compare the effects of peroxynitrite and NO treatments of rhIRP1, the protein was also reacted with the fast NO-releasing donor DEA−NONOate under strict anaerobic conditions. Optical spectra were recorded over time, and after incubation for 45 min, biological activities and the RR spectrum were determined. In the optical spectra shown in Figure 5A, the broad band characteristic of the $[4Fe\text{-}4S]^{2+}$ clusters around 400 nm was rapidly replaced by one band at ca. 350 nm indicating cluster perturbation. After purification of the reaction mixture by heparin affinity chromatography, the recovered colorless protein exhibited the spectrum given in Figure 5A (dotted line). The RR spectrum (Figure 5B, bottom trace) did not exhibit the typical features of the Fe−S cluster in the 300−400 cm^{-1} spectral range; aconitase activity was essentially lost (more than 85% inhibition), and interestingly, the IRE binding capacity was almost as high as that found by including 2% 2-ME (full activity) in the assays (Figure 5C). Altogether, these results indicate that, unlike peroxynitrite, anaerobically handled NO quantitatively converts [4Fe-4S]-rhIRP1 into the apoprotein that is able to bind IREs. Moreover, rhIRP1 exposed to NO did not react with anti-nitrotyrosine antibodies (Figure 5D).

DISCUSSION

To distinguish the respective effects of peroxynitrite and NO on IRP1, we analyzed the post-translational modifications they induce in purified human recombinant IRP1 using resonance Raman in parallel to measurement of its biological activities. IRP1 was exposed to peroxynitrite synthesized using different protocols. In the first series of experiments, the results demonstrate the conversion of the native $[4Fe\text{-}4S]^{2+}$ cluster to a $[3Fe\text{-}4S]^+$ cluster in peroxynitrite-treated rhIRP1, which, as stated earlier, is responsible for the loss of aconitase activity, and still precludes mRNA binding.

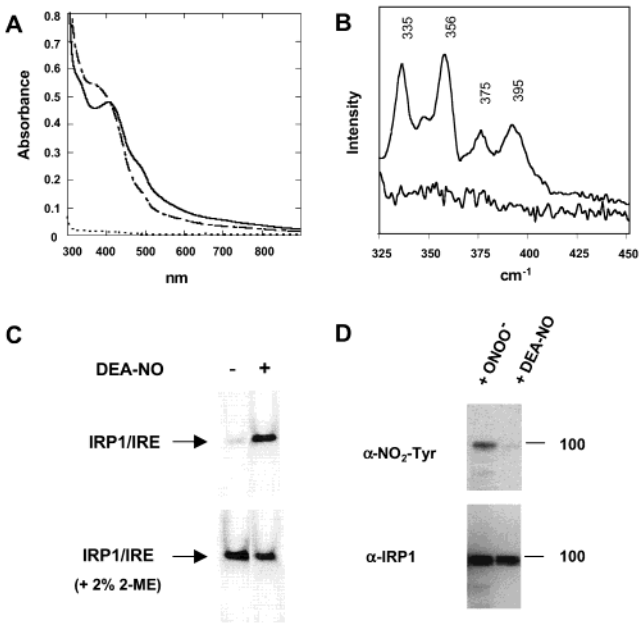

FIGURE 5: Conversion of [4Fe-4S] rhIRP1 into IRE-binding apoprotein by DEA-NO. Optical spectra of rhIRP1 before (—) and after (— - —) reaction with a 30-fold molar excess of DEA-NO. After separation of the reaction mixture on a heparin affinity chromatography column, rhIRP1 did not show any significant absorbance in the visible range (•••) (A). RR spectra of rhIRP1 before (top) and after (bottom) reaction with DEA-NO (B). Band shift assays of rhIRP1 before (left) and after (right) reaction with DEA-NO. Assays shown in the lower panel were supplemented with 2% 2-mercaptoethanol to develop the full activity of the samples (C). Western blot analysis of DEA-NO-treated rhIRP. Analysis was performed first with a monoclonal anti-nitrotyrosine antibody (top panel). Western blot analyses of peroxynitrite (solution B)-treated IRP1 are shown for comparison. The same blot was then stripped and reprobed with a polyclonal anti-IRP1 antibody to show that equal levels of IRP1 proteins were present in each sample (bottom panel) (D).

Thus, the mechanism by which peroxynitrite action inhibits aconitase activity of rhIRP1 is limited to removal of one Fe atom in the cluster (presumably the labile iron, Fe_a, which is the site of iso/citrate binding), as a minimal alteration of the enzyme. This conversion is reminiscent of the effects of H_2O_2 described by Brazzolotto et al. (*22*), but it is unlikely that the residual H_2O_2 content of peroxynitrite solution A, which was carefully controlled (less than 2%), played a role in the inhibition observed here. Indeed, the H_2O_2:rhIRP1 ratio in our experiments was 5 times lower than that used in ref *22*. In brief, in this series of experiments, the effect of peroxynitrite, solution A, on rhIRP1 in leading to inactivation of aconitase activity clearly appears to be essentially cluster conversion by labile iron removal without observable nitration of the protein.

The second series of experiments using a preparation of peroxynitrite prepared by a different procedure (solution B) confirmed the above data, but the reason peroxynitrite solution B was more effective in nitrating rhIRP1 is intriguing. Peroxynitrite and protein concentrations were both higher in this series of experiments, and because metals facilitate formation of phenol ring nitration by peroxynitrite (*17*), it was attractive to speculate that iron released from the Fe—S cluster upon peroxynitrite action catalyzed stronger self-nitration of rhIRP1. Also, nitrite ion can generate $NO_2^{\bullet}$ in the presence of a metal center (*35*), and as stated above, iron from the rhIRP1 Fe—S cluster may catalyze this oxidation. However, recent results from our laboratory showed that nitration was as significant in a mutant apo-IRP1 lacking the two cluster ligands C503 and C506 as in the wild-type holoprotein (E. Soum and J.-C. Drapier, unpublished observations). Alternatively, the nitrite content of peroxynitrite was also much higher in solution B than in solution A, and it is possible that partnership of nitrite with peroxynitrite is a critical parameter. Indeed, formation of nitrogen dioxide radical ($NO_2^{\bullet}$), the nitrating species, could be enhanced by the reaction between nitrite and carbonate radical ($CO_3^{-\bullet}$) which easily is derived from a reactive nitrosoperoxocarbonate ($ONOOCO_2^-$), a product from the reaction of peroxynitrite and CO_2 which would be dissolved in the buffer (*36*). In brief, the cooperation between peroxynitrite and nitrite, two NO-derived molecules which often coexist under pathophysiological conditions, may be crucial for determining IRP1 modification. In this regard, recent results from our laboratory indicate that intact cells, upon proper stimulation, can express nitrated IRP1 (C. Bouton and J.-C. Drapier, unpublished observations).

With regard to the effect of NO, our results extend previous data obtained with mitochondrial and cytosolic aconitases exposed to spermine-NONOate (*10*). An EPR study showed that NO targets the IRP1 [Fe—S] cluster with loss of aconitase activity, but RNA binding capacity following NO or peroxynitrite treatments was not reported. Here, we performed gel shift experiments in parallel with the RR study, and we provide evidence that NO in the absence of oxygen can activate IRP1 IRE binding activity. The properties of the labile Fe_a in the aconitase Fe—S cluster as a Lewis acid suggest that it can oxidize NO to a species with a nitrosonium character. As previously discussed by Gardner et al. (*37*), such a reactant would attack nucleophilic groups, including thiol sulfurs, and facilitate the degradation of the aconitase cluster (*37*). Moreover, the same species, as a strong nitrosating compound, is also expected to modify nucleophilic protein side chains, as previously observed with other Fe—S proteins (*38*). It is therefore remarkable that rhIRP1 keeps its full IRE binding activity after reaction with DEA-NONOate, implying either that rhIRP1 does not exhibit side chain residue modifications or that modifications do not preclude the regulatory function of the protein. This observation is at variance with that made after peroxynitrite treatment. In the latter case, RR spectroscopy has been instrumental in revealing (i) that formation of a [3Fe-4S] cluster from the initial [4Fe-4S] one with loss of aconitase activity is an early event after peroxynitrite action and (ii) that tyrosine nitration of rhIRP1 is a result of significant peroxynitrite exposure. These two events are not necessarily coupled, and on the basis of our previous studies, it is likely that the ultimate form of IRP1 that resulted in prolonged or severe exposure to peroxynitrite is an apoprotein with at least oxidized Cys 437 preventing binding to IRE motifs (*12*). Furthermore, peroxynitrite-mediated nitration of IRP1 may be responsible for the impairment in binding mRNA, in an irreversible manner even in the presence of a reductant, as we previously reported (*39*). In contrast, reaction between rhIRP1 and NO did not provide evidence for any identified intermediate in the degradation of the cluster under the conditions that were used, except for some dinitrosyl iron species (results not shown). More importantly, this reaction

disclosed the full RNA binding capacity of the protein rather than signs of irreversible loss.

From a chemical perspective, the intrinsic reactivity of NO and that of peroxynitrite may be discriminated by the special IRP1 active site(s). On one hand, NO and its likely derivative with nitrosonium-like properties (see above) are expected to target efficiently the electron-rich Fe−S cluster and, possibly, the ensuing free cysteines. Such an NO-modified IRP1, which may include *S*-nitroso-IRP1, would remain, as long as a NO flux lasts, potentially able to interact with available IRE. As many *S*-nitrosothiols are labile, we can expect NO to be released from IRP1 nitrosated cysteine(s), after stopping the NO flux. Then, in a suitable redox environment, IRP1 would bind IREs as the apoprotein (*40*). These features bear many characteristics of a protection mechanism of the RNA binding function of IRP1 under sustained NO fluxes. On the other hand, peroxynitrite, as a strongly oxidizing anion, or other reactive nitrogen species, such as nitrogen dioxide, can interact with amino acid side chains at the IRP1 active site that contain several cationic residues that are important for IRE binding (*41*−*44*). Hence, the IRP1 active site may represent a favorable local environment for triggering peroxynitrite-mediated nitration, and it is tempting to propose that Tyr 501, which is very close to cysteines 503 and 506 holding the Fe−S cluster of IRP1 and belongs to the IRE binding domain (*45*), may represent a steric hindrance once nitrated. Further experiments, including mass spectrometry, will be required to identify the site(s) whose nitration potentially hampers IRE binding.

In conclusion, the results presented herein have important bearings on the physiological consequences of the interaction between IRP1 and reactive nitrogen species. This study confirms the ability of NO to efficiently activate IRP1, whereas peroxynitrite would break the regulatory pathway(s) dependent on the protein. It thus follows that IRP1 is a genuine target of NO acting as a messenger molecule, whereas conditions leading to peroxynitrite generation, with or without nitration, would represent a far more stressful situation for this system and for the cell as a whole.

ACKNOWLEDGMENT

We thank Marie-Jeanne Chauveau for skillful technical assistance. We acknowledge Dr. Claire Ducrocq (ICSN-CNRS, Gif-sur-Yvette, France) and Dr. Michel Lepoivre (BBMPC, Université de Paris-Sud, Orsay, France) for providing peroxynitrite solutions.

REFERENCES

1. Boldt, D. H. (1999) *Am. J. Med. Sci. 318*, 207−212.
2. Eisenstein, R. S. (2000) *Annu. Rev. Nutr. 20*, 627−662.
3. Beinert, H., Kennedy, M. C., and Stout, C. D. (1996) *Chem. Rev. 96*, 2335−2374.
4. Drapier, J. C., Hirling, H., Wietzerbin, J., Kaldy, P., and Kühn, L. C. (1993) *EMBO J. 12*, 3643−3649.
5. Weiss, G., Goossen, B., Doppler, W., Fuchs, D., Pantopoulos, K., Werner-Felmayer, G., Wachter, H., and Hentze, M. W. (1993) *EMBO J. 12*, 3651−3657.
6. Bouton, C. (1999) *Cell. Mol. Life Sci. 55*, 1043−1053.
7. Hanson, E. S., and Leibold, E. A. (1999) *Gene Expression 7*, 367−376.
8. Castro, L., Rodriguez, M., and Radi, R. (1994) *J. Biol. Chem. 269*, 29409−29415.
9. Hausladen, A., and Fridovich, I. (1994) *J. Biol. Chem. 269*, 29405−29408.
10. Kennedy, M. C., Antholine, W. E., and Beinert, H. (1997) *J. Biol. Chem. 272*, 20340−20347.
11. Castro, L. A., Robalinho, R. L., Cayota, A., Meneghini, R., and Radi, R. (1998) *Arch. Biochem. Biophys. 359*, 215−224.
12. Bouton, C., Hirling, H., and Drapier, J. C. (1997) *J. Biol. Chem. 272*, 19969−19975.
13. Cairo, G., Ronchi, R., Recalcati, S., Campanella, A., and Minotti, G. (2002) *Biochemistry 41*, 7435−7442.
14. Quaroni, L., and Smith, W. E. (1999) *Biospectroscopy 5*, S71−S76.
15. Greenacre, S. A., and Ischiropoulos, H. (2001) *Free Radical Res. 4*, 541−581.
16. Ischiropoulos, H. (1998) *Arch. Biochem. Biophys. 356*, 1−11.
17. Beckman, J. S., Ischiropoulos, H., Zhu, L., van der Woerd, M., Smith, C., Chen, J., Harrison, J., Martin, J. C., and Tsai, M. (1992) *Arch. Biochem. Biophys. 298*, 438−445.
18. Pfeiffer, S., Lass, A., Schmidt, K., and Mayer, B. (2001) *J. Biol. Chem. 276*, 34051−34058.
19. Gaut, J. P., Byun, J., Tran, H. D., Lauber, W. M., Carroll, J. A., Hotchkiss, R. S., Belaaouaj, A., and Heinecke, J. W. (2002) *J. Clin. Invest. 109*, 1311−1319.
20. Thomas, D. D., Espey, M. G., Vitek, M. P., Miranda, K. M., and Wink, D. A. (2002) *Proc. Natl. Acad. Sci. U.S.A. 99*, 12691−12696.
21. Kilpatrick, L. T. K., Kennedy, M. C., Beinert, H., Czernuszewicz, D. Q., Qiu, D., and Spiro, T. G. (1994) *J. Am. Chem. Soc. 116*, 4053−4061.
22. Brazzolotto, X., Gaillard, J., Pantopoulos, K., Hentze, M. W., and Moulis, J. M. (1999) *J. Biol. Chem. 274*, 21625−21630.
23. Beckman, J. S., Chen, J., Ischiropoulos, H., and Crow, J. P. (1994) *Methods Enzymol. 233*, 229−240.
24. Beckman, J. S., Beckman, T. W., Chen, J., Marshall, P. A., and Freeman, B. A. (1990) *Proc. Natl. Acad. Sci. U.S.A. 87*, 1620−1624.
25. Pick, E., and Keisari, Y. (1980) *J. Immunol. Methods 38*, 161−170.
26. Uppu, R. M., and Pryor, W. A. (1996) *Anal. Biochem. 236*, 242−249.
27. Drapier, J. C., and Hibbs, J. B., Jr. (1996) *Methods Enzymol. 269*, 26−36.
28. Leibold, E. A., and Munro, H. N. (1988) *Proc. Natl. Acad. Sci. U.S.A. 85*, 2171−2175.
29. Bouton, C., Chauveau, M. J., Lazereg, S., and Drapier, J. C. (2002) *J. Biol. Chem. 277*, 31220−31227.
30. Spiro, T. G., Czernuszwicz, R. S., and Han, S. (1988) in *Biological Applications of Raman Spectroscopy* (Spiro, T. G., Ed.) pp 523−553, John Wiley and Sons, New York.
31. Meyer, J., Moulis, J. M., Gaillard, J., and Lutz, M. (1992) *Adv. Inorg. Chem. 38*, 73−115.
32. Spiro, T. G., and Czernuszwicz, R. S. (2000) in *Physical Methods in Bioinorganic Chemistry* (Que, L., Jr., Ed.) Vol. 3, pp 59−119, University Science Books, Sausalito, CA.
33. Johnson, M. K., Czernuszewicz, R. S., Spiro, T. G., Ramsay, R. R., and Singer, T. P. (1983) *J. Biol. Chem. 258*, 12771−12774.
34. Ischiropoulos, H., Zhu, L., Chen, J., Tsai, M., Martin, J. C., Smith, C. D., and Beckman, J. S. (1992) *Arch. Biochem. Biophys. 298*, 431−437.
35. Vesela, A., and Wilhelm, J. (2002) *Physiol. Res. 51*, 335−339.
36. Groves, J. T. (1999) *Curr. Opin. Chem. Biol. 3*, 226−235.
37. Gardner, P. R., Costantino, G., Szabo, C., and Salzman, A. L. (1997) *J. Biol. Chem. 272*, 25071−25076.
38. Foster, M. W., and Cowan, J. A. (1999) *J. Am. Chem. Soc. 121*, 4093−4100.
39. Soum, E., and Drapier, J. C. (2003) *J. Biol. Inorg. Chem. 8*, 226−232.
40. Oliveira, L., Bouton, C., and Drapier, J. C. (1999) *J. Biol. Chem. 274*, 516−521.
41. Philpott, C. C., Klausner, R. D., and Rouault, T. A. (1994) *Proc. Natl. Acad. Sci. U.S.A. 91*, 7321−7325.
42. Butt, J., Kim, H. Y., Basilion, J. P., Cohen, S., Iwai, K., Philpott, C. C., Altschul, S., Klausner, R. D., and Rouault, T. A. (1996) *Proc. Natl. Acad. Sci. U.S.A. 93*, 4345−4349.
43. Kaldy, P., Menotti, E., Moret, R., and Kühn, L. C. (1999) *EMBO J. 18*, 6073−6083.
44. Gegout, V., Schlegl, J., Schlager, B., Hentze, M. W., Reinbolt, J., Ehresmann, B., Ehresmann, C., and Romby, P. (1999) *J. Biol. Chem. 274*, 15052−15058.
45. Swenson, G. R., and Walden, W. E. (1994) *Nucleic Acids Res. 22*, 2627−2633.

BI030041I